AN EXPERIMENTAL STUDY OF HEAT TRANSFER TO FLOWING GRANULAR MEDIA

Thesis by

Jan Karel Spelt

In Partial Fulfillment of the Requirements

for the Degree of

Mechanical Engineer

California Institute of Technology

Pasadena, California

1982

ACKNOWLEDGMENTS

The author wishes to express his sincere appreciation to Dr. C. Brennen and Dr. R.H. Sabersky for their advice and support during the course of this study. Thanks are also due to Mr. Elmer Szombathy and Mr. Fred MacDonald for their excellent work in the construction of the experimental apparatus.

This research was sponsored by grants from the National Science Foundation (Grant #CME 7915132) and from the Union Carbide Corporation. The generosity of their contribution is gratefully acknowledged.

Abstract

The convective heat transfer to a flowing, cohesionless granular material has been studied experimentally. Heat-transfer rates were measured for two materials from a heated plate installed in the floor of an inclined, open chute. The variable parameters were the bed depth and the mass flow rate.

At relatively small flow rates the heat-transfer rate increased with velocity in agreement with earlier studies. As the mass flow rate continued to rise however, it was discovered that the heat-transfer coefficient for a given bed depth reached a maximum and then decreased.

TABLE OF CONTENTS

LIST OF TABLES

LIST OF FIGURES

Nomenclature

A	Cross-sectional area of flow
d	particle diameter
h	depth of flow over center of heated plate; in.
$\bar{h}$	average heat-transfer coefficient
k	thermal conductivity of bulk granular material in the critical state
k_g	thermal conductivity of interstitial gas
L	length of constant temperature plate
$\dot{m}$	mass flow rate; lb/s
$\overline{Nu}_d^*$	Sullivan's average Nusselt number based on d and k_g
P	heater power density given by $\frac{V^2}{R} \frac{1}{\text{Heater Area}}$; $\frac{W}{in^2}$
Pe_L^*	Sullivan's modified Péclet number
R	resistance of heater
T	temperature
U	average velocity of flow
V	voltage across heating element
α	thermal diffusivity of bulk granular material in the critical state
ΔT_3	temperature difference between plate trailing edge and upstream flow; ^oF
ΔT_4	temperature difference between the middle of the plate and upstream flow; ^oF
ΔT_5	temperature difference between plate leading edge and upstream flow; ^oF.
ΔT_6	temperature difference between upstream flow and ambient temperature of 73^oF; ^oF

ΔT difference between the average plate temperature and either that of the flow or, in the case of a stationary bed, the ambient temperature; ^{o}F

ρ density of the bulk granular material in the critical state

θ angle of chute inclination; deg.

ν solids volume fraction

I INTRODUCTION

There is a twofold motivation for the present study concerning the heat-transfer characteristics of a flowing granular material. Firstly, certain industrial processing operations make use of equipment designed to heat or cool granular flows. Since very little is known about the behavior of such flows, there may exist means of improving the effectiveness with which they are handled. Secondly, from a more theoretical standpoint, measurements of the heat-transfer coefficient may lead to a better understanding of how the bulk density at the wall depends on various parameters of the flow. This expectation is based on the assumption that the heat-transfer rate and the local bulk density near the surface are closely related.

II HEAT TRANSFER TO FLOWING GRANULAR MATERIALS

The present investigation was concerned with the heat transfer to a granular material flowing in an inclined chute. For comparison it is pertinent to consider certain previous studies of heat transfer to flowing granular materials.

Sullivan [1] examined the behavior of a constant-temperature plate immersed in the flow of various granular materials within a vertical channel. He modelled his results by considering the granular material as a continuum with a special thermal resistance at the wall. The value of this wall resistance, which was imagined to result from pure conduction through a thin gas layer, was determined empirically by curve fitting. It was found to be equivalent to an air gap of about 1/10 of a particle diameter. The correlation derived from this model agreed well with the experimental results; furthermore it included the effect of particle diameter, bulk thermal conductivity and diffusivity as well as the plate length and the thermal conductivity of the interstitial gas. Figure II.1 shows these results of Sullivan. The coordinates are modified Nusselt and Péclet numbers defined as,

$$\overline{Nu^*_d} = \frac{\bar{h}\, d}{k_g}$$

$$Pe^*_L = \left(\frac{k}{k_g}\right)^2 \left(\frac{d}{L}\right)^2 \frac{uL}{\alpha} \quad .$$

A number of other investigators have noted results similar to those of Sullivan. Harakas and Beatty [2] as well as Dunsky et al [3] measured the heat transfer from constant temperature plates immersed in rotating packed beds of granular material. Their observations of the effect of

particle diameter and residence time at the plate (defined as plate length divided by particle speed) are qualitatively the same as those of Sullivan. That is, an increase in the average heat-transfer coefficient as the residence time decreases and/or the particle diameter decreases. In addition, Harakas and Beatty varied the interstitial gas within the packed bed and found that the bed may be modelled as a homogeneous continuum for sufficiently long residence times, small particle diameters and high effective thermal diffusivities of the bulk.

Ernst [4] examined the heat transfer to a confined flow of granular material while varying the velocity of a superimposed counterflow of the interstitial gas. His observations of the effect of particle diameter and residence time are in agreement with those made later by the aforementioned authors. Ernst noted only a small decrease in the heat-transfer coefficient for a given residence time as the velocity of the interstitial gas was increased in the direction opposite to that of the bulk flow.

Perhaps the most interesting studies, from the point of view of the present work, have been done by Botterill et al. Botterill and Butt [5] studied the heat-transfer characteristics of a flowing granular media as a means of better understanding the limiting factors in fluidized bed heat transfer. The motivation for this approach lies in the relatively accurate control of the particle residence time which is possible in a flowing packed bed experiment. These results, obtained in an apparatus similar to that of Sullivan's, qualitatively confirm the dependence of the heat-transfer coefficient on residence time and on particle diameter. In addition however, Botterill [6] briefly mentions that the heat-transfer coefficient reached a maximum and then decreased as the velocity of the

flow was increased. As a possible explanation he suggests that this may have been due to "wall effects and/or looser particle packing at the higher solids flowrates". This seems to have been the first time such a maximum was observed.

Botterill [6] attempted to use a discrete particle model to explain his results but found it necessary (as did Sullivan) to introduce at the wall a hypothetical gas film of thickness equal to about 10% of the particle diameter. This provided a good fit of the data for intermediate ranges of particle velocity but did not adequately model the observed behavior at very low or very high velocities (beyond the observed maxima). Botterill concluded that it would be necessary to allow for an effective gas film of varying thickness in order to fit the data over the entire range of velocities.

On the question of the physical reality of the gas gap at the wall, Botterill and Desai [7] propose that it is probably represented by an "effective gap" resulting from packing defects and particle interactions near the wall. They also describe experiments in which a surface-mounted thermistor detector was used to record the minute transient temperature fluctuations produced by passing particles. This work suggested that "considerably less than half" of the particles at the wall moving past the detector actually touched the surface. It also seemed to confirm the expectation that the particle packing near the wall was a function of the shape of the particles.

In addition to flowing packed beds, Desai did experiments with freely fluidized beds [8]. He found that for comparable particle residence times the heat-transfer coefficients for the flowing packed beds

were generally 25% higher than those for the fluidized beds. This was explained in terms of the denser particle packing which was believed to exist near the wall of the flowing packed bed.

Botterill concludes [7] that the particle packing density and the freedom of the particles near the wall are important factors governing the heat transfer to a fluidized or flowing packed bed. Not until these parameters are included, according to Botterill, will any model of the heat-transfer process be complete. This observation has special relevance to the present work.

Of the many attempts that have been made to model the heat transfer to gas fluidized beds, one of the most successful is the one by Kubie and Broughton [9]. In their model, packets of material from the bed are swept to the heat-transfer surface where transient conduction occurs for the time of packet residence. Allowance is made for the variation of the void fraction within a distance of one particle diameter from the surface. This is an important feature of the model as it permits the bulk density and thermal conductivity to vary according to some specified voidage distribution function in the vicinity of the wall. The effective conductivity of a packet of given voidage was computed using the method of Kunii and Smith [10]. It was found that for the voidage distribution assumed to exist in a bed of uniform spherical particles, the thermophysical properties of the bulk changed very rapidly with distance from the surface.

Comparisons between the Kubie and Broughton model and the moving packed bed data Harakas and Beatty [2], Desai [8], Butt [5] and others show a good agreement. However, this model is not directly applicable to the present work because of the current inability to relate the voidage distribution to parameters such as the flow rate and bed depth. Important

experimental and theoretical work in this area was done by Bagnold [12] who considered the Couette flow of dispersions of neutrally buoyant particles. He discovered that the particles generate a normal or dispersive force which is proportional to the shear stress. In flows having a free surface, such dispersive forces will produce changes in the void fraction. Bagnold also showed that the shear stress component, τ, due to the influence of the particles (as opposed to that caused by viscosity of the fluid) could be expressed as

$$\tau = f(\nu)\rho_p d^2\left(\frac{\partial u}{\partial y}\right)^2 \quad .$$

Here $f(\nu)$ is some undetermined function of the solids volume fraction ν, $\partial u/\partial y$ is the shear rate and ρ_p and d are respectively the density and diameter of the particles. Attempts to find the function $f(\nu)$ have been only partially successful and not without some recourse to empiricism. Some of the more recent work in this area has been done by Savage and Cowin [13] and by Savage and Jeffrey [14]. In the latter study the authors developed a statistical mechanical model which assumes that momentum transport is due to impulsive particle collisions. This theory predicts that the normal and shear stresses are proportional to the square of the particle diameter and the square of the shear rate as well as being strongly dependent on the solids volume fraction. The model is still in its early stages of development but seems to agree at least qualitatively with the experimental results of Bagnold. The impact of these functional relations upon the heat transfer to a granular material remains to be investigated.

III. EXPERIMENTAL PROGRAM

A. Introduction

The purpose of the experimental program was to extend Sullivan's heat transfer data to higher Péclet numbers. This was of interest since it appeared as if the Nusselt number, $\overline{Nu}_d^*$, was approaching an asymptote as Pe_L^* increased (Fig. II.1). By mounting a heated-plate assembly in the floor of an open chute, it was possible to measure the heat-transfer rates at particle velocities significantly higher than those observed by Sullivan in his small vertical duct.

B. Apparatus

The chute which was constructed for this investigation is shown schematically in Fig. III.1. The width of 3 in. was chosen to ensure negligible wall boundary layer effects in the midsection of the flow. Observations have indicated that such wall effects extend at most 0.5 in. inward from each wall. The length of 4 ft. was selected to yield essentially constant flow depths toward the end of the chute over the range of the anticipated mass flow rates.

The floor of the chute was constructed of aluminum and connected to an electrical ground to minimize the buildup of static charge within the flowing granular materials. Previous work had shown that this could be a problem affecting the reproducibility of results. Other grounded metal surfaces in the system were the storage bin, the supply hopper and both copper plates on the upper heating element. The heated plate was grounded via one of the leading edge thermocouple wires.

The heating element could be installed with setscrews in one of two cutout sections along the chute (see Fig. III.2). Care was taken to

ensure that the plate was installed flush with the floor of the chute to minimize disturbance to the flow. Likewise, the plastic tape used to close the air gap surrounding the plate was periodically replaced whenever it appeared as if the edges were beginning to fray.

Glass windows upstream of each cutout location allowed for the possibility of direct measurement of particle speed. When not in use, the alternate cutout was plugged with a close-fitting aluminum plate.

A heated-plate length of 2.5 in. was selected to give a range of Pe_L^* which would provide a good overlap with Sullivan's data while also allowing a significant extension of his $\overline{Nu_d^*}$ curve.

The chute was positioned by a clamp which could be moved along the two cantilevered support arms extending from the hopper stand. It was found that at low angles of inclination the mass flow rate was extremely sensitive to the precise chute angle. It thus became necessary to construct a special protractor capable of measuring the inclination to better than 1/4 degree.

The depth of the flow over the middle of the plate was measured with a point probe. Two small pieces of duct tape laminated to the ends of the probe were of use in the mustard seed experiments where, because of the size of the particles, it was not possible to observe the track of the probe tip in the surface of the flow. The probe was positioned so that 1/4 turn (0.02 in.) up or down either eliminated particle collisions with the duct tape or caused them to be continuous.

The heat transfer element is shown in Fig. III.3. A guard heater on the bottom of the 0.25 in. thick phenolic block prevented the downward loss of heat from the upper heater. The total heat loss from the top

heating element was thus assumed to be transferred either into the flow or horizontally to the air gaps. The heated plate was constructed of 0.032 in. thick copper. It was located in the middle portion of the heating element to eliminate edge effects on at least three sides. Surrounding the plate was another 0.032 in. thick copper plate which served to maintain a level surface. The plate heating element and the guard heater were 2" x 6", 50 W ribbon heaters manufactured by Sierracin/Thermal Systems. They were chosen because they are of an etched-foil construction which enhances the uniformity of the surface heat flux. This is important if the results are to be quantitatively accurate since it is assumed that the total power output of the central copper plate is simply

$$\frac{\text{Area of Plate}}{\text{Area of Heater}} \times \text{Heater Power} \quad .$$

The variation of heater resistance with temperature was checked and found to be less that 1 Ω per 50^{o}F; a change of 0.4%. This correction was neglected in the calculation of power output.

The electrical connections are shown in Fig. III.4. The two heating elements were separately powered by 120V A.C. variable autotransformers to facilitate the independent adjustment of the guard heater temperature.

All thermocouples used in the element were 0.005 in. chromel-alumel wire with a 0.003 in. thick Teflon insulation. Chromel-alumel was selected because of its relatively low thermal conductivity. This, combined with the small wire diameter and the fact that the wires are approximately isothermal in the vicinity of each junction, helped to minimize the perturbation error. In other words the measured temperature at each junction was probably very close to that which would have existed in the absence of the

thermocouples.

For the purposes of the present work it was thought sufficient to calibrate a single thermocouple in a water bath. The results are listed in Table III.1 along with the National Bureau of Standards (N.B.S.) reference data for chromel-alumel. The agreement between the calibration results and the N.B.S. data is very good. In the present experiments only small differences in temperature (less than $50^{o}F$) were measured. For this reason all of the thermocouple voltages have been converted to temperature differences using the constant factor 44 $^{o}F/mV$. This is the average temperature - EMF slope over the range of temperatures encountered in the present experiments.

To establish the correct guard-heater power, the temperatures on the top and bottom of the phenolic block (Fig. III.3) were measured using a welded-bead junction which was cemented into a shallow, 0.011 in. diameter hole. The wires to these junctions were led through 0.011 in. square grooves milled into the phenolic surfaces in order to allow the heating elements to lie flat.

The temperature of the flow upstream of the plate was measured with a simple twisted-junction thermocouple supported by a wire probe. To avoid disturbing the flow over the plate this probe was removed after each measurement. The temperature of the flow was found to be independent of the probe's exact position or depth of immersion.

The three thermocouples on the heated copper plate were of the series-junction type. The chromel and alumel wires were welded separately to the copper so that the plate formed part of each circuit. The temperature indicated by such a junction is the average of the actual temperatures

at the two points of contact. The thermocouple wires were again led away from the junctions through 0.011 in. square grooves milled into the copper. This ensured a uniformly close interface between the copper and the heater surface.

All of the thermocouples were connected to a rotary switch mounted in an insulated box (Fig. III.4). The voltages, which were read directly with a microvoltmeter, were thus porportional to the differences between the junction temperature and the temperature within the switch box.

C. Granular Materials

The experiments were conducted with two of the granular materials used by Sullivan; namely the glass traffic beads and the mustard seed. From Sullivan's plot of $\overline{Nu}_d^*$ vs Pe_L^* (Fig. II.1) it is evident that these two materials provide the widest possible range of Pe_L^*. Thus the glass traffic beads were used to obtain data at relatively low Pe_L^* thereby providing an overlap with Sullivan's results, while the mustard seed gave higher values of Pe_L^* and permitted the extension of data well beyond Sullivan's limit of $Pe_L^* = 5000$.

To avoid reproducing the measurement of the thermal diffusivity and heat capacity, both the glass beads and the mustard seed were obtained from the same sources used by Sullivan as well as by Pearce [11]. The glass traffic beads (P - 0170) were purchased from Potters Industries, Inc., Hasbrouk Heights, N.J. The whole mustard seed (w311) came from McCormick and Co., Inc. Baltimore, M.D. A rough check on the similarity between these materials and those used in the earlier studies, was made by determining the bulk density and the distribution of particle diameters. The mustard seed diameter was measured using a pair of calipers while

the glass beads were measured with a light microscope fitted with an eyepiece graticule. Although neither the mustard seed nor the glass beads were perfectly spherical, it is clear that if sufficient "diameters" are randomly measured, the average value will be representative of the sample. The bulk density in the critical state (loosely packed as if the material were flowing) was obtained using the technique outlined by Pearce [11]. A sample of the material was placed into a graduated cylinder of known weight. The cylinder was then capped and slowly inverted several times to create a loose packing. The volume and weight of the sample were then measured to give the critical bulk density.

The results of these tests along with the other critical data from Pearce are presented in Table III.2. It was concluded that the materials were sufficiently similar so that the previous data could be used to evaluate the present experiments.

D. Experimental Procedure and Related Observations

A single experiment in this investigation began with the establishment of a steady state heat flow between the heated copper plate and a flowing bed of granular material of a specific depth. Prior to each experiment, an antistatic fluid (MS-166 Enstat, Miller-Stephenson Chemical Co. Inc.) was applied to all of the electrically insulated surfaces within the chute; specifically the plexiglass side walls, the glass windows in the floor of the chute and the plastic tape closing the air gaps around the heating element. This precaution along with the grounding of all metallic surfaces seemed to eliminate electrostatic effects, and perhaps as a result the reproducibility of the data was excellent.

An experiment was begun by fully opening the main gate from the

hopper and establishing a flow of approximately the desired mass flow rate and depth. The upper heater was then set to some predetermined voltage to give a plate temperature 27^{o} to 50^{o}F above that of the flow. The guard heater was then roughly set to give the desired temperature balance across the phenolic block. While the heaters were warming up, the inclination of the chute and the height of the control gate were adjusted to yield the desired mass flow at the particular depth under study. The mass flow rate was measured by simply using a stopwatch to record the time required to fill a container held at the end of the chute. The container and the material were then weighed on one of two balances depending upon the total mass collected. If over 20 lbs. were obtained in the timing period a large scale accurate to ± 0.25 lb. was used. Smaller amounts were weighed on a 6 kg. capacity balance having a full-scale accuracy of 1%.

Having established the flow rate and depth, the voltage across the guard heater was carefully adjusted to give a temperature difference of less than 0.5 ^{o}F across the phenolic. A complete set of thermocouple voltages were then recorded and the mass flow rate was remeasured. Periodically during the course of an experiment it became necessary to make minor adjustments in the control gate height and the guard heater voltage. Such adjustments were followed by further sets of voltage and mass flow readings at approximately 3 minute intervals until it became apparent that a steady state had been attained. The total time required for a single experiment varied between roughly 15 and 30 minutes, during which time the supply hopper was intermittently refilled.

As a matter of reference, the room temperature (usually constant

at 73^{o}F) and the relative humidity were recorded as were semiquantitative observations of the flow behavior. For example, the location of the transitions between plug and shear flows were measured relative to the plate position. It was felt that such features of the flow may have an effect on the rate of heat transfer.

Three distinct sets of experiments were undertaken in this work. Glass beads and mustard seed were used with the plate installed in the downstream location and another set of mustard seed experiments were conducted with the plate in the upstream position. In each of these, the depth of the flow was varied between a lower limit set by the particle diameter and the degree of saltation in the flow and an upper limit resulting from practical limitations on the rate at which the hopper could be refilled. In order to obtain very low flow rates at a given depth, some of the mustard seed experiments (#48,49,51,52,54,55 and 62) at the downstream location were conducted with an aluminum plate clamped over the end of the chute. This plate essentially formed a weir over which the mustard seed had to flow. And although it extended at most two seed diameters above the chute floor, it effectively backed up the mustard seed producing a very uniform plug flow over the heated copper plate. These plug flows were in contrast to the usual shear flows encountered in all of the other experiments. The end plate was not used with glass beads nor when the heated plate was at the upstream location.

A number of experiments were also performed with stationary beds of varying depth. These provided a sort of baseline from which the relative effects of each flow could be gauged.

Despite the fact that the plastic tape closing the air gaps around

the heating element had a thickness of only 0.005 in., at high velocities and shallow flow depths it could disturb the flows of both mustard seed and glass beads. Although these disturbances disappeared a short distance downstream, it was uncertain at times if a normal flow was completely restored over the plate. This problem was corrected by extending the tape 5 in. upstream of the leading edge of the plate thereby triggering the disturbances further upstream.

In most of the experiments the flow over the plate was shearing to some degree. Often this meant that the flow had "yielded" some distance upstream of the plate and had undergone a transition from a plug flow to one of much greater shear. Such a transition was characterized by a marked increase in the slope of the free surface as the flow accelerated and became shallower. Some experiments were performed to try and detect differences in the heat-transfer properties of shear and plug flows. However, the range of Pe_L^* and depth over which these experiments could be conducted was severely restricted. Practical difficulties were encountered in trying to establish both shear and plug flows of the same depth by means of the plate clamped to the end of the chute. In fact it may be impossible to achieve this precise condition since it is not clear at this time what factors determine the formation of one or the other type of flow. Experiments #51 and #52 (mustard seed, downstream location) represent plug flows of 0.30 in. depth induced by means of the end plate. Experiment #53 was performed with the end plate removed. Apparently the shear flow at this relatively shallow depth has a slightly greater Nusselt number. On the other hand, the 0.75 in. deep plug flow experiments #48, #49 and #55 seem to yield results similar to the shear flows

of the same depth. Although these results are not conclusive, it would seem at this point that the Nusselt number is not strongly affected by the character of the flow (plug or shear).

A curious and as yet unexplained phenomenon which was noticed primarily with the mustard seed, was the slow but steady increase in the mass flow rate throughout any experiment at low Pe_L^* . In one case, the mass flow rose monotonically from 0.043 lb/s to 0.074 lb/s (an increase of 72%) over a period of 1 1/4 hours. This occurred without any adjustment of the gate height and without any discernible change in the depth of the flow over the plate. As was mentioned earlier, this phenomenon was a regular occurrence only with mustard seed at the lowest Pe_L^* experiments for each flow depth. Because of this it became necessary to carefully match each mass flow reading with a complete set of temperature and power measurements. It was found that the plate temperatures changed slowly enough so that they could be accurately associated with an average mass flow over some time interval.

The depth of the flow over the 2.5 in. length of the heated plate was generally quite uniform. Two types of variation were noticed: Small random fluctuations in the depth and a steady state slope in the free surface. The former was almost always less that $\pm$ 0.02 in. while the latter was at most a decrease of 1/8 in. over the plate length.

E. Calculations and Error Estimate

The data from the three main sets of experiments as well as those for the stationary beds are shown in Tables III.3,4 and 5. Table III.5 also gives the results for an experiment in which the plate was completely uncovered and cooled only by natural convection to the surrounding

atmosphere. These tables list the results in terms of Sullivan's modified Péclet and Nusselt numbers which are defined as

$$Pe_L^* = \left(\frac{k}{kg}\right)^2\left(\frac{d}{L}\right)^2 \frac{uL}{\alpha}$$

$$\overline{Nu_d^*} = \frac{\bar{h}d}{k_g} \quad .$$

Here, $u = \frac{\dot{m}}{\rho A}$

and $$h = \frac{V^2}{R} \cdot \frac{\text{Plate Area}}{\text{Total Heater Area}} \cdot \frac{1}{\Delta T\ (\text{Plate Area})}$$

$$= \frac{V^2}{R \cdot \Delta T \cdot (\text{Total Heater Area})} \quad .$$

In these calculations $R = 253\ \Omega$ and Total Heater Area = 12 in^2. ΔT is taken as the difference between the upstream flow temperature and the average of the three temperatures along the copper plate.

The following are the major sources of error in the determination of $\overline{Nu_d^*}$:

- variations in the heater resistance
- random fluctuations in the voltage applied to the heater
- heat loss across the air gaps surrounding the element
- vertical heat flux either downward away from the flow or upward from the guard heater
- nonuniform heat flux over the surface of the heater

The relative errors in the values used for the heater resistance and voltage are both quite small (0.3% and 0.6% respectively) and may be neglected.

The error produced by heat flux across the air gaps surrounding the phenolic block may be estimated by assuming pure conduction through the gap. Then,

$$q = \frac{1}{2} k_g \frac{\Delta T}{W}$$

where, because we are only interested in the heat loss from the top heater, a factor of 1/2 has been introduced. If the area $A = 5.47\ in^2$, $\Delta T = 50^oF$ (taking the maximum possible temperature difference) and the gap width $W = 1/8$ in, then $q = 0.40W$. This represents at most 2% of the total power output of the heater.

The maximum vertical heat flux between the two heaters across the phenolic block is given by

$$q = A k \frac{\Delta T}{t}$$

where $A = 12\ in^2$, $t = 0.25$ in, ΔT is at most 0.5^oF and for linen phenolic $k = 4.1 \times ;0^{-3} \frac{W}{in^oF}$. Thus $q = 0.10W$ or 0.5% of the total heater power.

Some uncertainty exists in how best to model the heated plate. Although it was constructed of copper, the temperature distributions along the plate are indicative of a constant heat flux surface rather than one of constant temperature. Substantial temperature gradients were induced in the plate by the flow and to a lesser extent by apparent inhomogeneities in the heat flux over the surface of the heating element. As expected for a plate of constant heat flux, the magnitude of these gradients varies with the flow conditions over the plate. This is evident upon consideration of the values of ΔT_3, ΔT_4 and ΔT_5 in Tables III.3, 4 and 5. These are respectively the trailing-edge, middle and

leading-edge plate temperatures relative to the flow temperature. On the basis of the stationary bed experiments, it appears as if inhomogeneities in the heating element output contribute only a relatively small amount to the temperature gradients. Most of the temperature differences are probably flow-induced. For example, the temperature difference along the plate covered by a stationary bed or exposed directly to the air is generally about $1^{o}F$. This is less than 4% of the difference between the average plate temperature and that of the ambient air. In the flowing bed however, there could be as much as an $11^{o}F$ difference the leading and trailing edges of the plate. This may be up to 39% of the difference between the average plate temperature and that of the flow. Examples of such extreme cases are the glass bead experiments #8, #19 and #25. Referring to Table III.3, note also that the temperature difference between the leading edge and the middle is usually about twice as large as that between the trailing edge and the middle. Both of these observations are consistent with a constant heat flux plate. Finally, if a linear temperature gradient is assumed to exist along the leading half of the plate, these data indicate that the maximum rate of heat conduction through the copper at any point is at most 9% of the assumed heat flux to the flow. Therefore only a relatively small amount of heat is redistributed along the plate. Most of the output of the heating element must be transferred directly through the copper plate to the flow in the manner of a constant heat flux surface. Therefore in summary, the behavior and magnitudes of the temperature gradients along the heated plate suggest that the plate is best characterized as a constant heat-flux surface.

Taking into account the various factors mentioned above, the overall accuracy of the average Nusselt number, $\overline{Nu}_d^*$, under the most unfavorable conditions is estimated to be $\pm 8\%$.

The reproducibility of these experiments was found to very good. With one exception, the data for a given bed depth were collected over a period of at least two days. Regardless of when they were obtained, most of the data points when plotted, lay close to smooth, similarly-shaped curves lending confidence to the repeatability. As an additional test, several points were accurately reproduced after an interval of two days (compare experiments #33, and #47; #71 and #73; #72 and #80).

F. Presentation of Results

The results of the present investigation are illustrated in Figs. III.5,6 and 7. Figures III.5 and 6 show the data points obtained with the heated plate at the downstream and upstream locations respectively. Figure III.7 shows some of Sullivan's data points plotted along with several of the curves of Fig. III.5. This provides a comparison of the ranges of Péclet number, Pe_L^*, investigated in the two studies and illustrates the typical scatter of Sullivan's data relative to the curve of his correlation.

Perhaps the most interesting aspect of the present study was the discovery that the heat-transfer coefficient in a granular flow may have a well-defined maximum as a function of the flow rate. Referring to Figs. III.5,6 and 7 it is evident that as the Péclet number, Pe_L^*, increases beyond the values encountered by Sullivan, each constant-depth curve reaches a maximum average Nusselt number, $\overline{Nu}_d^*$, and then begins to slope downward. In this region, the curves corresponding to the

larger depths generally lie above those for the lesser depths. This trend seems to be common to all of the experiments and may be a reflection of changes in the bulk density at the plate surface.

At relatively low values of Pe_L^*, the heat-transfer characteristics of the flows in the chute are similar to those encountered by Sullivan. All of the constant-depth curves in both plate locations tend to asymptotically approach or at least run parallel to Sullivan's correlation as Pe_L^* decreases. The small differences that do exist at low Pe_L^* can probably be attributed to dissimilarities in the apparatus, to experimental errors (Section III.E) or to slight differences in the properties of the granular materials (Section III.C). For example, recall that Sullivan employed a constant-temperature plate in a closed vertical duct. It seems reasonable that such an apparatus would yield results somewhat different to those coming from the present setup of a constant heat flux plate set into an open chute. Nevertheless, the agreement at low Pe_L^* between the present results and those of Sullivan is encouraging.

IV DISCUSSION AND CONCLUDING REMARKS

The main objective of the present investigation was to obtain heat-transfer data for granular flows of relatively high speed. The results are presented in Figs.III.5, 6 and 7. At lower values of the modified Péclet number, Pe^*_L, the trend of the present data appears to be similar to that observed by Sullivan. However, as Pe^*_L (and hence particle velocity) increases, a maximum Nusselt number, $\overline{Nu^*_d}$, is reached. This is then generally followed by a decrease in the heat-transfer rate as Pe^*_L is further increased. The magnitudes of $\overline{Nu^*_d}$ and Pe^*_L in the vicinity of each maximum appear to be directly related to the depth of the flow.

These observations came as something of a surprise. No previous work, except perhaps that by Botterill and Desai [7], had indicated that the heat-transfer coefficient could reach a maximum and then decrease with increasing flow rate. Indeed, such a result seems at first glance to be contrary to intuition. However, a plausible explanation can be put forward based on the competing effects of enhanced convection on the one hand and decreasing bulk density due to increasing shear rate on the other. It is proposed that as the flow velocity increases beyond a certain point the bulk density at the wall begins to decrease appreciably. This in turn lowers the bulk thermal conductivity and serves to counteract the increase in the rate of heat transfer due to the higher particle velocities. This hypothesis seems to fit the trends observed in the present data. For example, in the region of the maxima in Figs.III.5 and 6 it is seen that $\overline{Nu^*_d}$ generally increases with bed depth. This may be explained by assuming that the greater depths give rise to increased bulk densities and hence increased conductivities at the floor of the chute.

The concept of a variable bulk density in a granular flow was established experimentally by Bagnold [12]. As mentioned before he showed that the shear stress, τ, in a flowing granular material may be given by

$$\tau = f(\nu)\rho_p d^2\left(\frac{\partial u}{\partial y}\right)^2$$

where $f(\nu)$ is some unknown function of the solids volume fraction ν, ρ_p and d are respectively the particle density and diameter and $\partial u/\partial y$ is the shear rate. The precise form of the function $f(\nu)$ remains in doubt. It is thus not possible at this time to provide a more quantitative analysis of the trends in the present data. On the other hand, by providing a link between the density and the flow velocity, these heat-transfer data may perhaps be useful in helping to determine the function $f(\nu)$. This indeed was one of the motivations for the present work.

References

[1] Sullivan, W.N. and Sabersky, R.H., "Heat Transfer to Flowing Granular Media", Int. J. Heat Mass Transfer, vol. 18, 1975, pp.289.

[2] Harakas, N.K. and Beatty, K.O., "Moving Bed Heat Transfer: Effect of Interstitial Gas with Fine Particles", Chem Engng. Progr. Symp. Ser., vol. 59, no. 41, 1963, pp. 289.

[3] Dunsky, V.D., Zabrodsky, S.S. and Tamarin, A.I., "On the Mechanism of Heat Transfer Between a Surface and a Bed of Moving Particles", Proc. 3rd Int. Heat Transfer Conf., A.I. Ch.E., vol. 3, 1966, pp.293.

[4] Ernst, R., "Der Mechanismus des Wärmeüberganges an Wärmaustauschern in Fliessbetten (Wirbelschichten)", Chemie. Ingr. Tech., vol. 31, 1959, pp. 166.

[5] Butt, M.H.D., Ph.D. Thesis, Univ. of Birmingham, England, 1967.

[6] Botterill, J.S.M., Butt, M.H.D., Cain, G.L. and Redish, K.A., "The Effect of Gas and Solids Thermal Properties on the Rate of Heat Transfer to Gas-Fluidized Beds", Int. Symp. on Fluidization, Netherlands Univ. Press, Amsterdam, 1967, pp. 442.

[7] Botterill, J.S.M. and Desai, M., "Limiting Factors in Gas-Fluidized Bed Heat Transfer", Powder Technology, vol. 6, 1972.

[8] Desai, M., Ph.D. Thesis, Univ. of Birmingham, England, 1970.

[9] Kubie, J. and Broughton, J., "A Model of Heat Transfer in Gas-Fluidized Beds", Int. J. Heat Mass Transfer, vol. 18, 1975, pp. 289.

[10] Kunii, D. and Smith, J.M., "Heat Transfer Characteristics of Porous Rocks", A.I. Ch. E. J., vol. 6, no. 1, 1960, pp. 71.

[11] Pearce, J.C., "Mechanics of Flowing Granular Media", Ph.D. Thesis, Calif. Inst. of Tech., 1975.

[12] Bagnold, R.A., "Experiments on a Gravity-Free Dispersion of Large Solid Spheres in a Newtonian Fluid Under Shear", Proc. Roy. Soc., vol. A225, 1954, pp. 49.

[13] Savage, S.B., "Gravity Flow of Cohesionless Granular Materials in Chutes and Channels", J. Fluid Mech., vol. 92, part 1, 1979, pp. 53.

[14] Savage, S.B. and Jeffrey, D.J., "The Stress Tensor in a Granular Flow at High Shear Rates", accepted for publication J. Fluid Mech., 1981.

[15] National Bureau of Standards, "NBS Circular #561", 1955.

TABLE III.1 Temperature – voltage data for chromel – alumel thermocouples

Reference Tables[1]		Water Bath Test	
Temp Interval (°F)	Slope ΔT/Δ(EMF) (°F/mV)	Temp Interval	Slope ΔT/Δ(EMF) (°F/mV)
75-85	44.2	75-89	43.8
75-95	44.2	75-95	42.3
75-105	44.2	75-107	43.8
75-115	44.1	75-118	45.0
75-125	44.0	75-120	45.0
	ave = 44.1		ave = 44.0

[1]Reference [15]

TABLE III.2 Thermophysical properties of glass traffic beads and whole mustard seed[1]

Material	Bulk Specific Gravity	Mean Diam. (mils)	Stnd.Dev. Diam. (mils)	Thermal Diffusivity $\times 10^6$ (ft^2/s)	Thermal Conductivity (Btu/hr·ft·°F)
Glass Traffic Beads	1.46 1.46*	12.8 14.8*	1.6 1.0*	1.80	0.12
Mustard Seed	0.71 0.73*	81.4 80.9*	7.7 8.0*	0.86	0.08

[1]Data taken from Pearce [11] unless otherwise indicated.

*Value measured for present sample of material.

TABLE III.3 Experimental data for glass traffic beads obtained at the downstream plate location

Exp't	θ	h	$\dot{\bar{m}}$	P	ΔT_3	ΔT_4	ΔT_5	ΔT_6	ΔT	Pe^*_L	$\bar{Nu}^*_d$
96	-	0.15	0	0.209	37.0	36.5	35.6	-1.3	36.4	0	0.230
21	19.1	"	0.0832	4.13	38.3	33.4	23.8	0.9	31.8	78	5.20
20	19.5	"	0.130	4.16	33.4	29.5	21.6	1.3	29.3	121	5.64
31		"	0.190	4.15	33.0	29.0	22.9	0.4	28.2	177	5.88
22	20.8	"	0.348	4.15	34.3	31.2	26.4	1.3	30.6	325	5.40
30	22.3	"	0.484	3.38	31.2	29.5	25.5	0.9	28.7	452	4.72
23	23.7	"	0.656	4.12	42.7	40.9	37.4	1.3	40.3	612	4.08
29	25.6	"	0.828	3.35	37.4	37.0	34.8	1.3	36.4	773	3.68
24	32.5	"	1.15	0.996	24.6	24.6	22.9	1.3	24.0	1073	1.65
97	-	0.30	0	0.204	36.5	36.1	34.8	-1.3	35.9	0	0.227
10	19.0	"	0.178	4.13	38.3	32.6	24.2	0.9	31.4	83	5.20
8	20.0	"	0.390	4.15	33.0	29.5	22.4	0.0	28.4	182	5.84
13	20.5	"	0.60	4.15	31.7	28.2	22.4	1.8	27.4	280	6.04
11	20.5	"	0.941	4.15	32.1	29.0	23.3	1.3	28.3	439	5.88
5	21.0	"	1.16	4.12	33.4	30.4	24.2	0.0	29.3	541	5.60
6	23.0	"	1.72	4.12	36.1	33.4	28.2	0.4	32.6	803	5.00
7	25.0	"	2.25	4.14	40.0	37.8	33.0	0.9	37.0	1050	4.40
9	29.0	"	2.75	4.14	44.4	44.4	42.7	1.3	43.8	1280	3.74
98	-	0.60	0	0.208	39.6	39.6	38.7	-1.8	39.4	0	0.211
18	19.1	"	0.54	4.15	33.9	29.5	22.0	1.3	28.4	127	5.84
19		"	0.67	4.15	32.1	28.2	21.1	1.3	27.1	156	6.12
14	20.8	"	1.31	4.15	29.5	26.4	20.2	2.2	25.5	306	6.48
15	22.5	"	1.87	4.15	29.9	26.8	21.1	1.3	26.1	436	6.32
16	27.0	"	5.08	4.13	37.4	36.5	33.0	-1.3	35.6	1185	4.64

(continued next page)

TABLE III.3 (continued)

Exp't	θ	h	$\dot{\bar{m}}$	P	ΔT_3	ΔT_4	ΔT_5	ΔT_6	ΔT	Pe^*_L	$\overline{Nu}^*_d$
99	-	0.70	0	0.208	40.0	39.6	38.7	-1.8	39.4	0	0.211
25	20.6	"	1.15	4.10	29.9	26.8	19.8	0.4	25.5	230	6.40
26	21.0	"	1.34	4.15	29.5	26.4	19.8	0.9	25.2	268	6.56
27	21.8	"	2.15	4.15	29.0	26.4	20.2	1.8	24.9	430	6.68
28	23.0	"	3.10	4.15	31.7	29.0	23.8	0.0	25.9	620	6.40

TABLE III.4 Experimental data for mustard seed at the downstream plate location.

Exp't	θ	h	$\dot{\bar{m}}$	P	ΔT_3	ΔT_4	ΔT_5	ΔT_6	ΔT	Pe^*_L	$\bar{Nu}^*_d$
92	-	0.3	0	0.133	27.3	26.8	26.4	-1.8	26.8	0	1.09
40	15.1	"	0.037	1.61	38.3	36.1	32.1		35.4	966	9.96
51	16.7	"	0.047	1.62	40.9	38.7	34.3		38.0	1220	9.33
52	16.6	"	0.056	1.64	39.6	37.4	33.4	-1.3	36.9	1470	9.72
53	15.5	"	0.063	1.60	36.1	33.9	30.4	-0.9	33.4	1650	10.5
43	16.5	"	0.077	1.61	34.3	32.6	29.0		31.9	2030	11.1
42	18.3	"	0.148	1.62	32.6	30.4	27.3		30.0	3880	11.8
41	18.8	"	0.207	1.61	32.6	30.8	27.7		30.4	5430	11.6
46	20.5	"	0.626	1.61	33.9	32.6	30.4		32.3	16400	10.9
39	21.3	"	0.732	1.61	34.8	33.4	31.2		33.3	19200	10.6
45		"	0.847	1.62	39.2	37.8	35.6		37.6	22200	9.44
44	24.8	"	0.964	1.62	43.6	42.7	40.5		42.2	25300	8.40
93	-	0.45	0	0.165	37.0	36.5	35.6	-2.2	36.4	0	0.99
62		"	0.063	1.70	42.2	40.0	36.1	-0.9	39.4	1100	9.44
60		"	0.102	1.62	37.8	36.1	32.6	-0.9	35.4	1790	10.0
58		"	0.265	1.65	35.2	33.4	29.9	-0.4	32.9	4640	11.0
64	18.7	"	0.337	1.63	33.4	31.7	28.2	-0.9	32.8	5900	11.6
63	19.9	"	0.777	1.63	31.2	29.5	26.8	0.4	29.3	13600	12.2
59	21.1	"	1.02	1.63	31.7	30.4	28.2	0.9	30.1	17900	11.9
61		"	1.56	1.63	36.1	35.2	33.4	0.9	34.9	27300	10.2
94	-	0.6	0	0.190	41.4	40.5	39.6	-1.8	40.3	0	1.03
54	12.0	"	0.020	1.63	51.0	48.4	43.6	-0.9	47.7	268	7.49
33	17.6	"	0.249	1.61	36.5	34.8	31.2	-0.4	34.2	3270	10.3
47	19.9	"	0.260	1.61	36.5	34.3	30.8		33.8	3410	10.4
37	19.0	"	0.377	1.60	35.6	33.9	30.8	0.0	33.5	4950	10.5
32	21.0	"	0.611	1.61	35.6	34.3	31.7	-0.9	33.6	8020	10.5
34	22.5	"	1.74	1.61	37.4	36.5	34.8	-0.4	36.2	22800	9.74
38	28.7	"	3.09	1.64	39.6	38.7	37.0		38.4	40600	9.35

TABLE III.4 (continued)

Exp't	θ	h	$\bar{\dot{m}}$	P	ΔT_3	ΔT_4	ΔT_5	ΔT_6	ΔT	Pe^*_L	$\bar{Nu}^*_d$
95	-	0.75	0	0.191	43.1	43.1	41.8	-2.6	42.7	0	0.98
55		"	0.023	1.61	53.2	50.6	45.3	-0.9	49.7	242	7.14
48	17.4	"	0.168	1.63	38.3	36.1	32.1		35.5	1760	10.0
49		"	0.432	1.63	35.2	33.4	29.5		32.7	4540	10.9
65	19.0	"	0.630	1.64	35.2	33.4	29.9	0.0	32.8	6620	11.0
57		"	0.755	1.64	34.8	33.4	29.9	-0.9	32.8	7930	11.0
50		"	2.58	1.61	33.9	32.6	30.4		32.2	27100	10.9

TABLE III.5 Experimental data for mustard seed obtained at the upstream plate location and for the uncovered plate.

Exp't	θ	h	$\dot{\bar{m}}$	P	ΔT_3	ΔT_4	ΔT_5	ΔT_6	ΔT	Pe^*_L	$\bar{Nu}^*_d$
92	-	0.3	0	0.133	27.3	26.8	26.4	-1.8	26.8	0	1.09
80	16.0	"	0.064	1.63	37.0	34.8	31.2	-0.4	34.4	1690	10.4
72	16.0	"	0.067	1.61	36.1	33.9	30.4	-0.9	33.5	1770	10.5
68	17.0	"	0.109	1.61	33.9	32.1	29.0	-1.3	31.7	2860	11.1
91	17.5	"	0.165	1.64	34.3	32.6	29.5	-0.9	32.1	4330	11.2
70	19.8	"	0.244	1.62	34.3	33.0	30.4	-0.9	32.6	6410	10.9
73	21.3	"	0.366	1.62	36.5	35.2	32.6	0.0	34.5	9630	10.3
71	21.3	"	0.367	1.62	36.1	34.8	32.1	-0.9	34.3	9640	10.3
69	28.0	"	0.547	1.20	30.4	29.9	27.7	0.9	29.6	14400	8.87
93	-	0.45	0	0.165	37.0	36.5	35.6	-2.2	36.4	0	0.99
78	16.7	"	0.155	1.63	37.0	34.8	31.2	-0.9	34.2	2710	10.4
75	17.0	"	0.286	1.60	34.3	33.0	29.5	-0.4	32.3	5010	10.8
74	21.3	"	0.542	1.63	34.3	32.6	29.5	0.0	32.1	9490	11.1
76	24.5	"	0.835	1.62	34.3	33.0	30.4	0.9		14600	11.0
77	31.6	"	1.17	1.62	35.2	33.9	32.1	1.8		20600	10.4
94	-	0.60	0	0.190	41.4	40.5	39.6	-1.8	40.3	0	1.03
84	15.5	"	0.168	1.62	37.8	35.6	31.7	0.0	35.1	2210	10.1
83	17.6	"	0.359	1.64	35.6	33.9	30.4	0.0	33.6	4710	10.6
79	21.0	"	0.734	1.64	34.8	33.0	29.5	-0.4	32.4	9640	11.1
81	29.7	"	1.52	1.63	33.9	32.6	29.9	2.6	31.8	20000	11.2
82	35.5	"	1.84	1.64	34.3	33.0	31.2	3.5	32.5	24200	11.0

TABLE III.5 (continued)

Exp't	θ	h	$\bar{\dot{m}}$	P	ΔT_3	ΔT_4	ΔT_5	ΔT_6	ΔT	Pe^*_L	$\bar{Nu}^*_d$
95	-	0.75	0	0.191	43.1	43.1	41.8	-2.6	42.7	0	0.98
88a	16.0	"	0.180	1.63	39.2	37.0	32.6	0.0	36.4	1890	9.81
88b	16.0	"	0.202	1.62	38.3	36.1	32.1	0.0	35.7	2120	9.94
85	19.1	"	0.672	1.65	35.6	33.9	29.9	-0.9	33.2	7060	10.9
86	25.5	"	1.57	1.63	33.4	31.7	29.0	0.0	31.3	16500	11.4
87	32.6	"	2.19	1.63	32.6	30.8	29.0	2.6	30.7	23000	11.6
56[1]	-	0	0	0.214	42.7	42.7	41.4	-0.9	42.5	0	1.10[2]

[1] uncovered plate.

[2] based on mustard seed diameter.

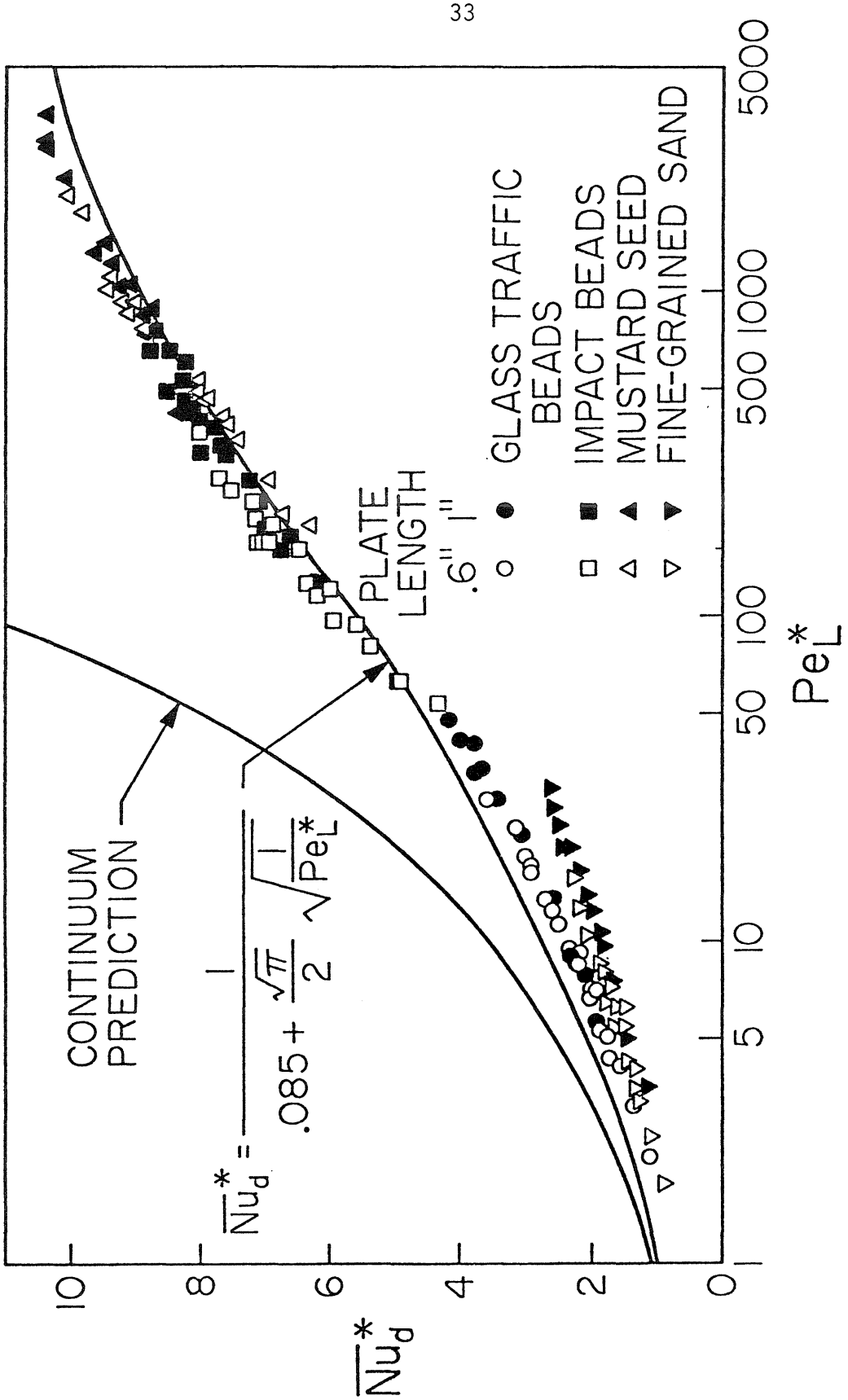

Fig.II.1 Sullivan's [1] data and proposed correlation. Modified Nusselt number as a function of modified Péclet number. Data for all materials tested and both plate lengths.

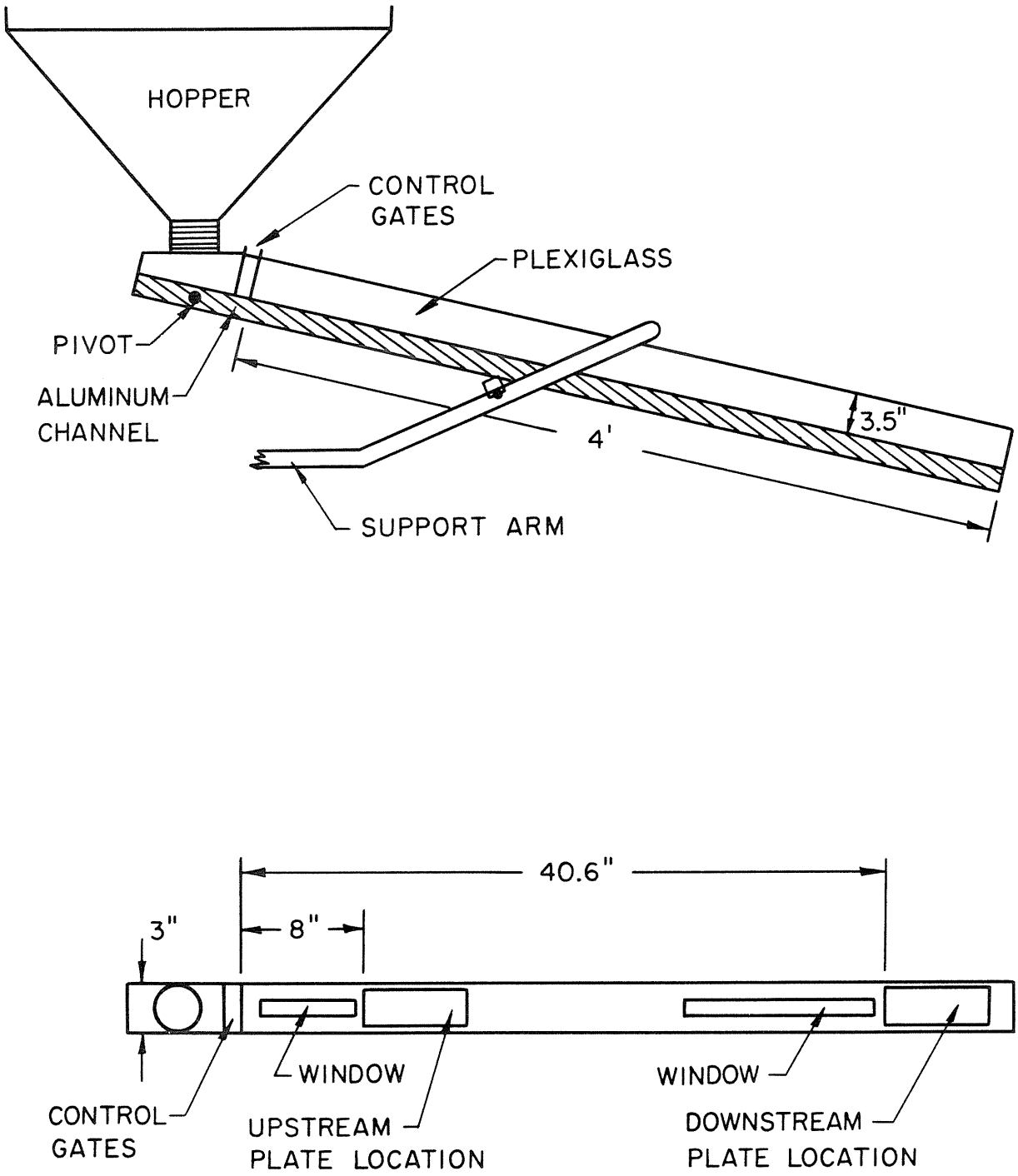

Fig.III.1 Side and top views of chute.

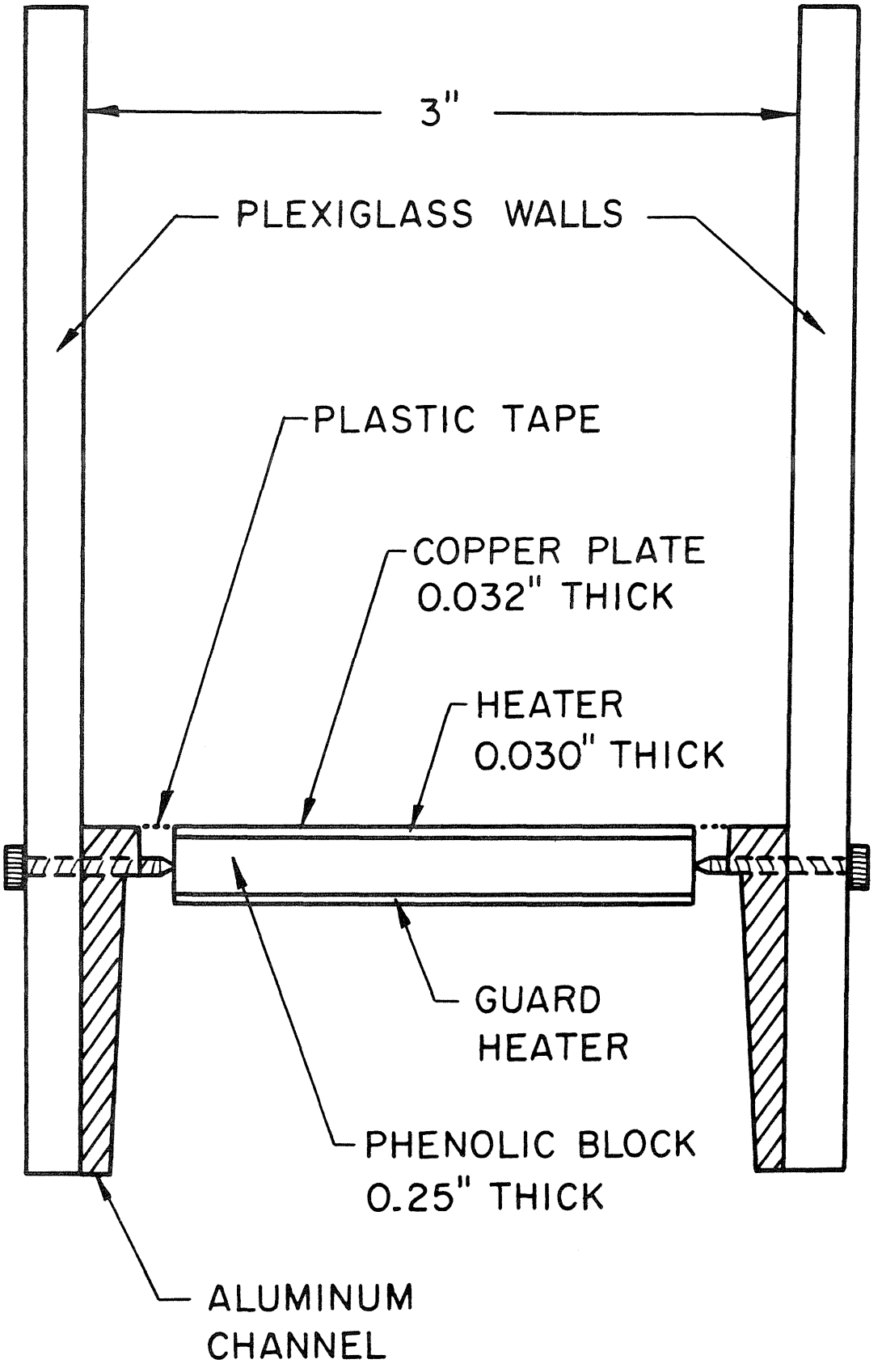

Fig.III.2 Cross-section of chute showing heating element installed.

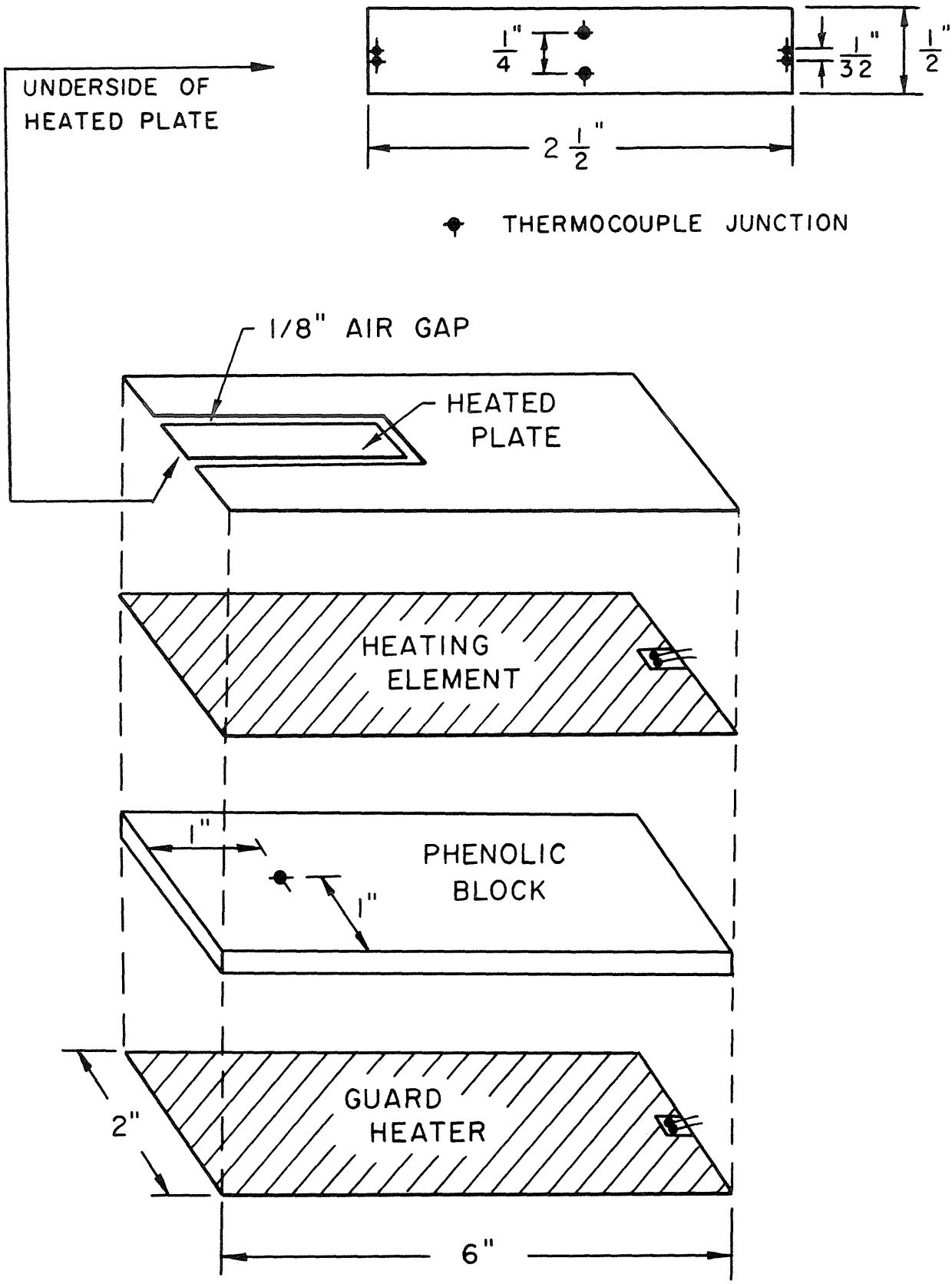

Fig.III.3 Heating element assembly showing positions of thermocouples.

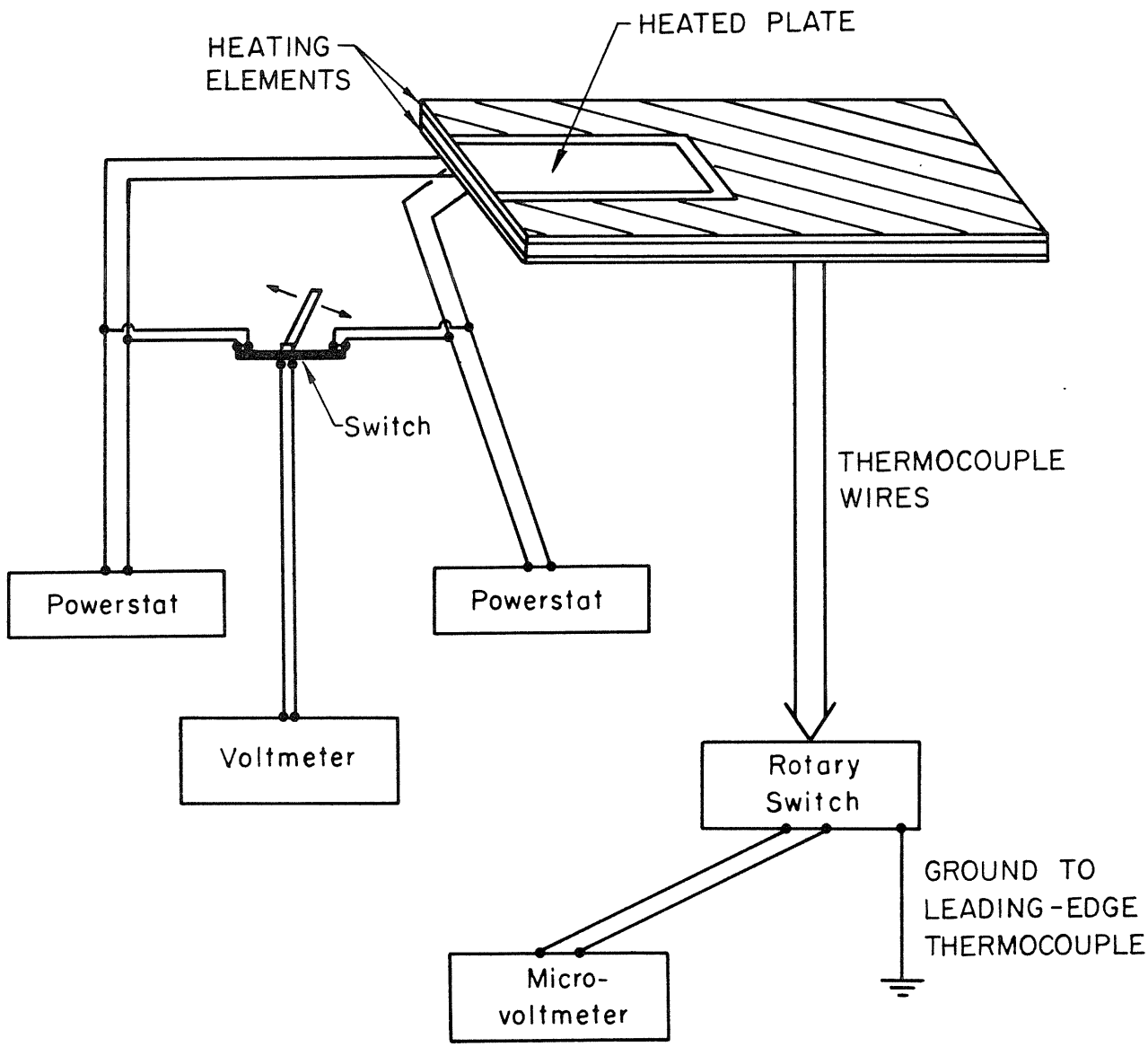

Fig.III.4 Schematic diagram of electrical connections.

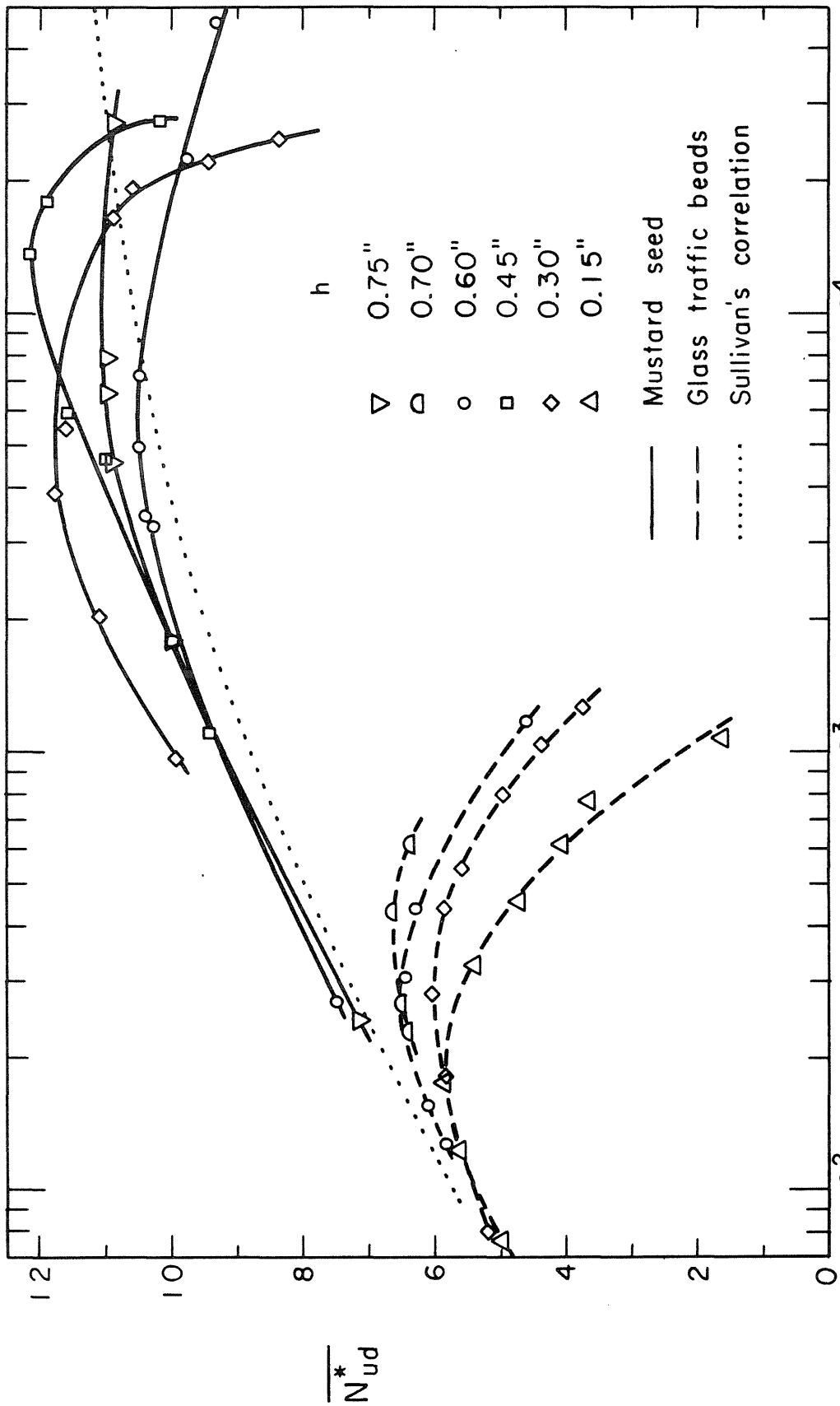

Fig.III.5 Modified Nusselt number as a function of modified Péclet number for the glass traffic beads and mustard seed at the downstream plate location.

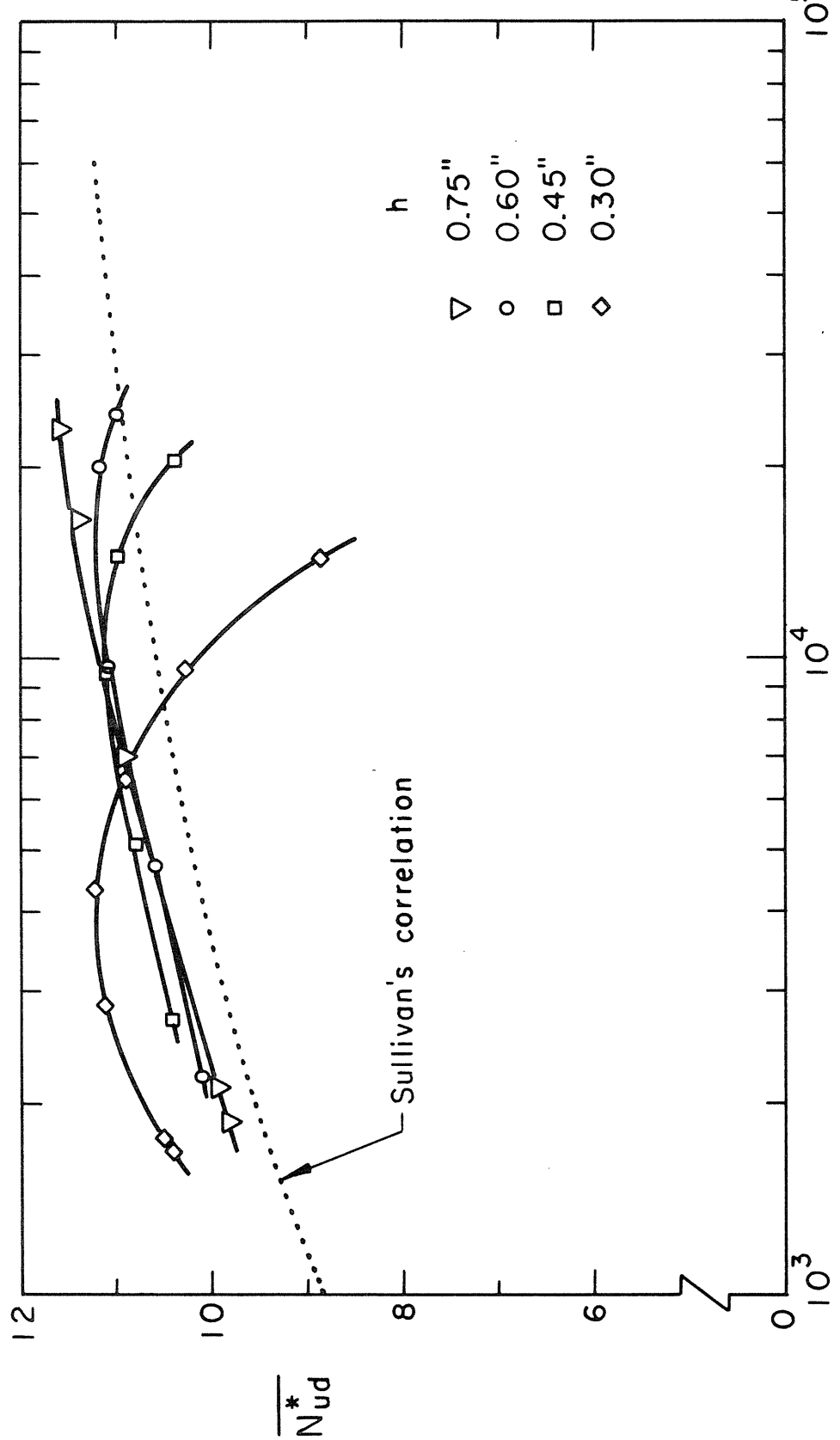

Fig.III.6 Modified Nusselt number as a function of modified Péclet number for the mustard seed at the upstream plate location.

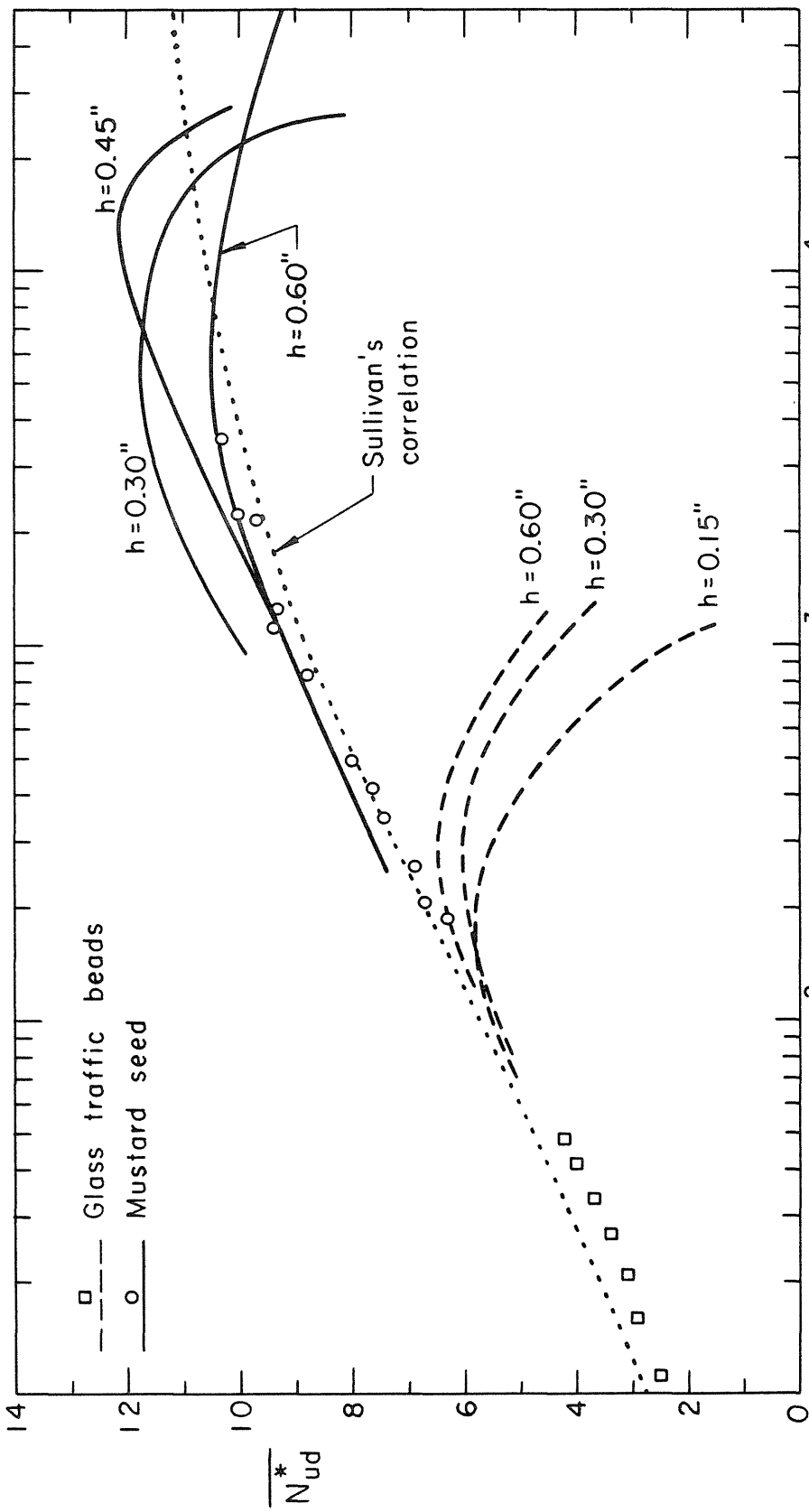

Fig.III.7 Modified Nusselt number as a function of modified Péclet number. Lines are curves through present data reproduced from Fig.III.5. Data points are from Sullivan [1].